5GV

UCRL 3174

UNIVERSITY OF CALIFORNIA

Radiation Laboratory

TWO-WEEK LOAN COPY

This is a Library Circulating Copy which may be borrowed for two weeks. For a personal retention copy, call Tech. Info. Division, Ext. 5545

BERKELEY, CALIFORNIA

DISCLAIMER

This document was prepared as an account of work sponsored by the United States Government. While this document is believed to contain correct information, neither the United States Government nor any agency thereof, nor the Regents of the University of California, nor any of their employees, makes any warranty, express or implied, or assumes any legal responsibility for the accuracy, completeness, or usefulness of any information, apparatus, product, or process disclosed, or represents that its use would not infringe privately owned rights. Reference herein to any specific commercial product, process, or service by its trade name, trademark, manufacturer, or otherwise, does not necessarily constitute or imply its endorsement, recommendation, or favoring by the United States Government or any agency thereof, or the Regents of the University of California. The views and opinions of authors expressed herein do not necessarily state or reflect those of the United States Government or any agency thereof or the Regents of the University of California.

UCRL-3174

UNIVERSITY OF CALIFORNIA
Radiation Laboratory
Berkeley, California

Contract No. W-7405-eng-48

ELASTIC AND INELASTIC SCATTERING OF 48-Mev ALPHA PARTICLES BY CARBON AND MAGNESIUM

Franklin J. Vaughn

(Thesis)

October 21, 1955

Printed for the U.S. Atomic Energy Commission

ELASTIC AND INELASTIC SCATTERING OF 48-Mev ALPHA PARTICLES BY CARBON AND MAGNESIUM

Contents

Abstract 3

I. Introduction 4

II. Experimental Method

General Procedure 6

The Alpha-Particle Beam and Beam-Alignment Procedures 9

Scattering Chamber, Vacuum System, Target Mechanism, Beam-Monitoring System, and Beam-Energy Determination 10

Counter, Absorber Changer, Electronics and Associated Controls 11

Targets 12

Measurement of Angular Distributions 12

III. Reduction of Data

Differential Cross Sections 19

Errors 22

IV. Results and Conclusions

Elastically Scattered Alpha Particles 29

Carbon target 29

Magnesium target 34

Inelastically Scattered Alpha Particles 36

General Considerations 36

Inelastic scattering from carbon 39

4.43-Mev level 39

7.65-Mev level 41

9.61-Mev level 43

Inelastic Scattering from Magnesium 45

Conclusions 47

Tables 48

Acknowledgments 56

References 57

ELASTIC AND INELASTIC SCATTERING OF 48-Mev ALPHA PARTICLES BY CARBON AND MAGNESIUM

Franklin J. Vaughn

Radiation Laboratory
University of California
Berkeley, California

October 21, 1955

ABSTRACT

The angular distributions of the differential cross sections for elastic scattering of 48-Mev alpha particles by carbon and magnesium have been measured. In addition, angular distributions of the differential cross sections for inelastically scattering alpha particles, leaving carbon in the 4.43-Mev, the 7.65-Mev, and the 9.61-Mev excited states and magnesium in the 1.368-Mev excited state have been determined.

In the elastic scattering, an attempt has been made to estimate the interaction radii from the separation of the maxima and minima of the observed angular distributions.

The distributions of the inelastically scattered alpha particles were all observed to be peaked in or near the forward direction, and all exhibit one or more secondary maxima at larger angles. An attempt has been made to fit the observed distributions by employing a slight modification of the Austern, Butler, and McManus direct interaction theory. This attempt has met with some success for alpha particles inelastically scattered from the lowest excited states of carbon and magnesium, but no agreement between theory and experiment was found for scattering from the two higher excited states of carbon.

I. INTRODUCTION

When a beam of high-energy particles (nucleons or nuclei) is directed at a thin target, two general types of processes occur. The first is elastic scattering, in which the beam particles emerge leaving the target nuclei in their ground states. The second includes inelastic scattering--in which the beam particles are emitted but the target nuclei are left in excited states--and nuclear reactions, as a result of which particles different from those in the bombarding beam emerge.

Various attempts have been made to fit observed angular distributions of elastically scattered protons and neutrons of energies from about 10 to 32 Mev. These attempts have usually involved the use of some sort of optical model of the nucleus. For example, Melkanoff, Nodvik, Saxon, and Woods[1,2] have fitted experimental data on the elastic scattering of 17- and 31-Mev protons and 14-Mev neutrons from various elements quite well by using a four parameter diffuse-surface optical model. Blair[3] has developed a semiclassical model in attempting to explain the angular distribution of elastic alpha particles from heavy elements. It has been applied with some success to the scattering of 22- and 48-Mev alpha particles from gold, lead, and silver; the work at 22 Mev was done by Wall, Rees, and Ford,[4] and that at 48 Mev by Ellis and Schecter.[5] Recently the angular distributions of 19- and 40-Mev alpha particles elastically scattered from aluminum have been determined. The work at 19 Mev was done by Bleuler and Tendam,[6] while that at 40 Mev was done by Eisberg, Igo, and Wegner.[7] No theoretical work, however, has been published on the elastic scattering of alpha particles of energies in this region from light elements.

Two types of theories have been applied to predict or explain angular distributions of inelastic particles and the products of nuclear reactions. The first of these, the compound-nucleus theory,[8] predicts angular distributions of the emitted particles which are symmetric about 90° in the center-of-mass system. The second type, which is based on what is usually termed direct or surface interactions, was first evolved by Butler[9] in attempting to explain observed angular

distributions of protons from (d, p) reactions. Later Huby and Newns[10] proposed a theory of the same general type to explain inelastic deuteron angular distributions. Austern, Butler, and McManus[11,2] formulated a theory that predicts the angular distribution of the products of (p, p'), (n, n'), (p, n) and (n, p) reactions. All these direct interaction theories yield angular distributions that are proportional to the squares, or sums of squares, of certain spherical Bessel functions, and are thus peaked in or near the forward direction. They also relate the distributions to the spins and parities of the initial and final nuclear states, and thus the observation of angular distributions forms a useful tool of nuclear spectroscopy in cases for which such theories are applicable.

Thus far there have been no experimental data published on angular distributions of inelastically scattered alpha particles, and no theory has been specifically applied to such processes. It was therefore thought that it might prove interesting and useful to measure some such angular distributions. This has been done in the experiment reported here. The absolute differential cross section has been determined as a function of angle for inelastic scattering of alpha particles from the first three excited states of C^{12} and from the first excited state of Mg^{24}. For carbon, the measurements extend from 7° to 90° in the laboratory system, while for magnesium they extend from 7° to 150°. At the same time, the angular distributions of 48-Mev alpha particles elastically scattered from carbon and magnesium have been found. In all cases observations were made at enough angles so that the detailed structure of the distributions would be apparent. Attempts have been made to apply existing theories and modifications thereof to explain some of the observed results.

II. EXPERIMENTAL METHOD

General Procedure

The equipment used and most of the experimental methods employed have already been described in detail by Fischer[12] and Ellis.[5] Therefore the description of the apparatus and procedures is given very briefly except where modifications or changes were made.

Figure 1 is a schematic diagram of the experimental arrangement. The 48-Mev alpha-particle beam produced by the 60-inch Crocker Laboratory cyclotron was brought out through the shielding and into a 36-inch-diameter scattering chamber. After passing through a thin target located in the center of this chamber, it was collected in a Faraday cup. The alpha particles scattered from the target were detected by a triple proportional counter telescope, the angular position of which with respect to the beam could be changed by remote control. Between the target and the counter was located a variable aluminum absorber. The arrangement of the counter and absorber changer is shown schematically in Fig. 2. By changing the amount of absorber through which the scattered particles had to pass before entering the counter, one could cause alpha particles of various energies to be counted. Thus at each angular setting of the counter, one could obtain the number of alpha particles counted per unit of charge collected as a function of absorber. When these data were plotted, the area under the observed peaks corresponding to the various elastic and inelastic groups of alphas could be measured. The target thickness and the solid angle subtended by the counter aperture were measured, and the "range bite" of the counter was determined. Thus all the information necessary for the calculation of the absolute differential cross sections at each angular position of the counter was obtained.

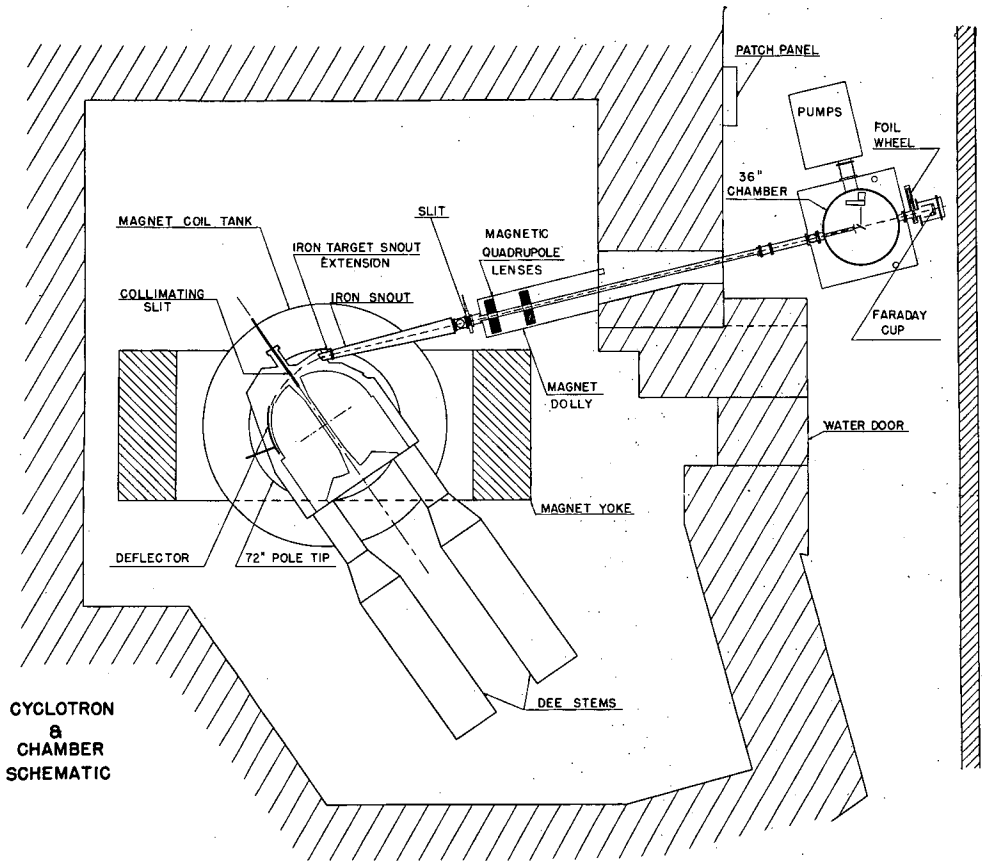

Fig. 1. Schematic diagram of the experimental arrangement.

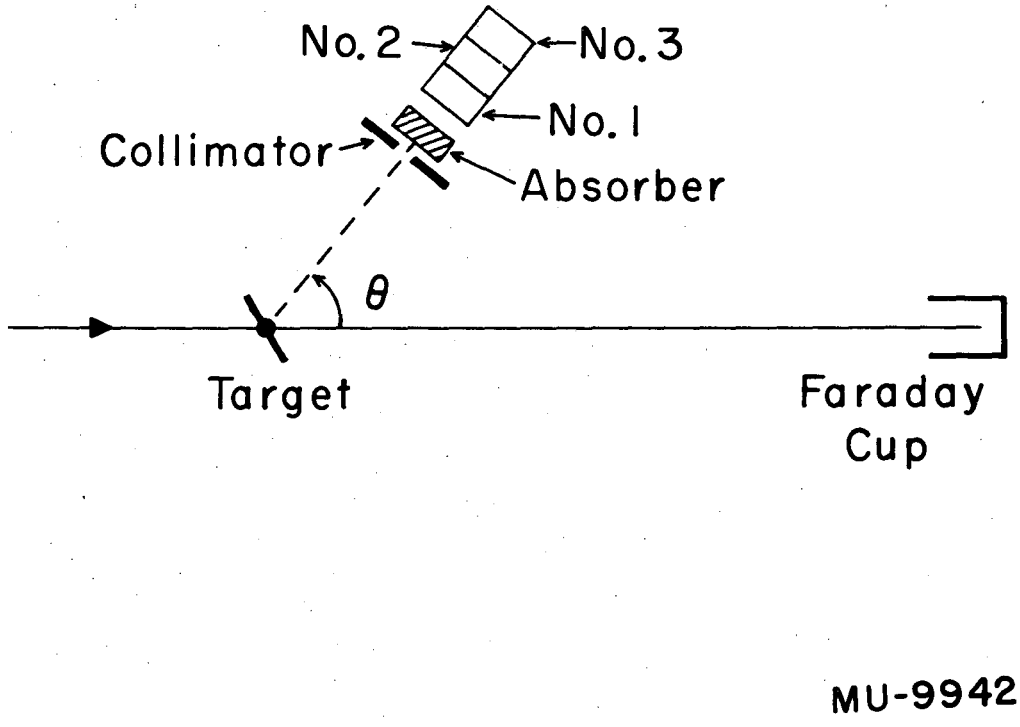

Fig. 2. Schematic diagram of the counter arrangement.

The Alpha-Particle Beam and Beam-Alignment Procedures

The beam used and the method of bringing it out and aligning the scattering chamber were as Ellis[5] has described. However, all runs were made with the beam collimators in place to avoid the possibility of slight changes in the beam position with oscillator power or other cyclotron variables. During the first run with a magnesium target, the collimators were used inside the chamber. For all other runs they were used externally, as it was found that the target-out background was thereby reduced to a negligible amount at all angles at which measurements were made. With the collimators used, the beam spot on the target was slightly greater than 1/8 inch in diameter.

The beam intensity used during the magnesium runs varied from about 10^{-9} ampere at the forward angles to about 10^{-7} ampere at the largest angles. During the carbon runs the beam intensity was kept below 2×10^{-8} ampere to avoid burning a hole through the polystyrene target.

The final step in the beam-alignment procedure was to measure the reading of the counter angle indicator with the counter directly in the beam. The indicator should then read a counter angle of 0°, and any deviation from that reading must be applied as a correction to the counter angle. This correction is a constant if the angle through which the counter has been moved from the forward direction is accurately shown by the counter position indicator. Checks were made and it was found that the indicated angular changes were accurate within 0.1 degree.

During the runs on magnesium, the beam position relative to the 10° position of the counter was measured in the manner used by Ellis.[5] This consisted in running the counter through a very small beam and determining the indicator reading for maximum beam in the counter. However, to employ this procedure the beam had to be reduced by a very large factor from its normal running level, and it was very difficult to maintain such a small beam while measurements were made.

Therefore two other procedures were devised and used during the carbon runs. The first involved the use of a stand containing a 1/16-inch vertical slit. This stand was accurately mounted on the table in a position 45° counterclockwise from the counter. With the beam at

normal running level, the stand was moved across the beam and the angle corresponding to maximum beam through the slot and into the Faraday cup was determined. The deviation of this reading from that which indicated the slot to be directly forward gave the desired correction factor.

Another method used to determine this correction was essentially the same as that used by Ellis[5] but with the advantage that a normal beam level could be used. This involved replacing the 1/4-inch-diameter collimator hole in front of the absorber changer (see Fig. 2) by one only 5 mils in diameter. This was done by mounting a small brass plate containing the 5-mil hole in place of the thinnest absorber in the absorber changer. The plate could be moved into a position with the center of the small hole directly behind the center of the 1/4-inch hole. Then the counter was run through the beam and the indicated angle corresponding to maximum beam through the hole noted. It was found that even the 5-mil hole admitted too many particles into the counter, so the number was reduced by inserting enough absorber in the absorber changer to stop a large fraction of the beam.

The results of these two methods of measuring the beam position agreed to better than 0.05°. For one carbon run the correction found was 0.23°, while for the other it was 0.12° in the other direction.

Scattering Chamber, Vacuum System, Target Mechanism, Beam-Monitoring System, and Beam-Energy Determination

The scattering chamber, vacuum system, target mechanism, and beam-monitoring system were as described by Ellis,[5] and the beam energy was measured in the same way. However, the beam energy was measured directly only once during each run. Thereafter the beam energy could readily be determined from the absorber thickness at which any elastic or inelastic peak was found.

From the plot of beam intensity into the Faraday cup versus absorber thickness, obtained during beam-energy determinations, one can find the energy spread in the beam as it emerges from the cyclotron. This is done by unfolding the theoretical energy spread produced

by range straggling and multiple Coulomb scattering from the observed spread. This was done several times and it was found that the full width at half maximum of the beam-energy distribution was about 500 kilovolts, or approximately 1%.

Counter, Absorber Changer, Electronics, and Associated Controls

The counter, electronics, and associated controls were those previously used and described by Ellis.[5] The absorber changer was also the same, but was not described by him, so a brief description is given here.

The absorber changer consisted of twelve Al absorbers contained in one unit and capable of independent movement by electromagnet into or out of the scattered beam. The thinnest absorber was 0.3005 mg/cm^2, and the others were accurate multiples of this unit, each twice as thick as the one preceding. Thus the thickest one was 615.4 mg/cm^2. In the front cover of the absorber changer was a 1/4-inch hole which determined the solid angle within which particles could enter the counter.

The position of the absorbers was controlled remotely from the counting area. Any combination could be inserted in the scattered beam, and those in the beam were indicated by lights. A small crystal microphone was clamped to the absorber changer, and the proper operation of the absorbers was indicated by clicks heard over a speaker when the absorbers were moved in or out.

Targets

The magnesium target used consisted of a rolled foil of normal relative isotopic abundance. Its thickness was about 1 mil.

Two carbon targets were used. One was cut from a 1-mil sheet of polystyrene $(CH)_n$. This target was very uniform and was used at all angles beyond 14°. Calculations showed that the peak resulting from the scattering of alpha particles from hydrogen would be detected at laboratory angles up to 14.5^o, so a graphite target was made for measurements at small angles. A 7.5-mil graphite sheet was obtained and a portion of it was carefully polished down to a thickness of about 2.5 mils. Since the thickness of such a target was not expected to be very uniform, it was used in only one position during the runs.

Measurement of Angular Distributions

As Ellis[5] has described, the coincidence circuits were set up to monitor both double coincidences between counter chambers No. 1 and No. 2 and triple coincidences between all three chambers. The difference between the two gives the number of particles that have stopped within the "range bite" of the counter. By the use of anticoincidence circuits, the number of particles counter in chambers No. 1 and No. 2 but not in chamber No. 3 was also indicated on a scaler. However, this figure was used only as a check, as it was found that the anticoincidence circuits were not very reliable. If the desired figure was the number of particles that had stopped within the range bite, it was

always determined by recording the numbers of double coincidences and triple coincidences and subtracting one from the other.

After the beam-energy determination, done at the beginning of each run, a thin gold target was placed in the beam and the counter was set at some convenient angle, usually 30° from the beam direction. The elastic peak was then located approximately by varying the absorber in the absorber changer until the difference between the double and triple coincidences per unit charge collected was a maximum. With the absorber at which this maximum was found inserted, pulses from the three chambers were observed on an oscilloscope and the high voltage and linear-amplifier gain for each chamber adjusted until the mean pulse height was about 50 volts.

Then the elastic peak was located exactly by plotting doubles minus triples against absorber thickness, the same charge being collected at each absorber setting. The absorber corresponding to the elastic peak was left in and discriminator curves were run for the first two counter chambers. Typical discriminator curves are shown in Fig. 3, and the voltages at which the discriminator biases would be set at this step of the procedure are indicated. It should be noted that there is no real plateau on the discriminator curve for chamber No. 2 because the particles in that chamber are very near the ends of their ranges. The discriminator bias for chamber No. 3 was always set low, usually about 7.5 volts, so that any pulse above the noise level would be counted.

The discriminator biases were now left at the settings determined from the curves and a spectrum of the gold elastic peak was obtained by plotting doubles minus triples against absorber thickness for a fixed amount of charge collected at each value of absorber thickness. This type of spectrum will be called a differential range spectrum. Then the discriminator bias voltages for chambers No. 1 and No. 2 were lowered to about 15 or 20 volts. An absorber thickness about 20 mg/cm^2 less than that corresponding to the elastic peak was inserted. With this absorber in, all the particles elastically scattered from the target and which entered the hole in front of the absorber changer would make pulses high enough to be counted in all three chambers. Increasing the absorber in small steps and determining the number

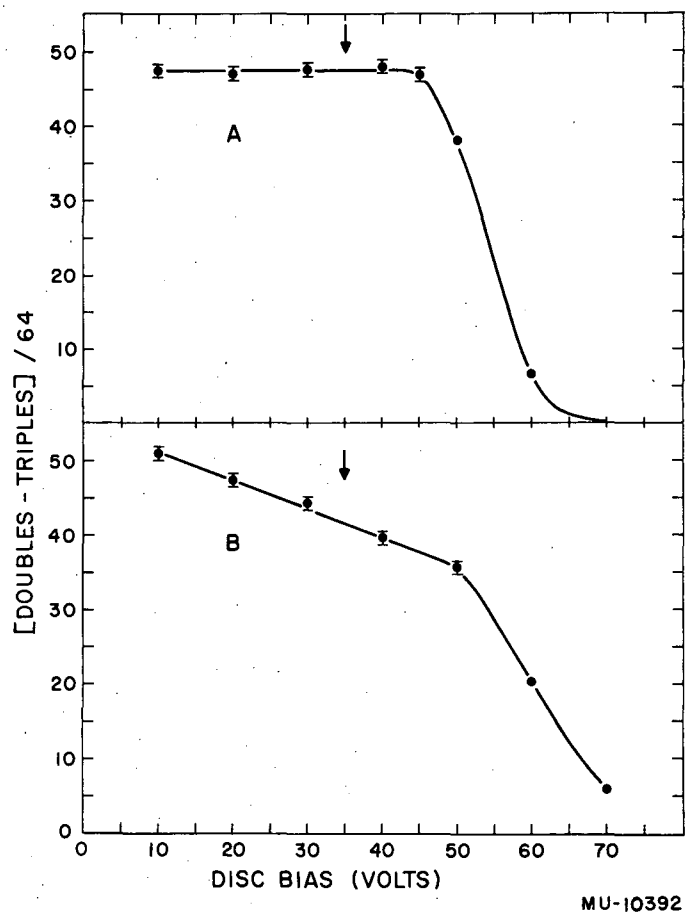

Fig. 3. Typical discriminator curves, obtained with alpha particles on Au and the counter at 30°. A is for counter chamber No. 1, the bias on chamber No. 2 being 20 volts and that on chamber No. 3 being 10 volts. B is for chamber No. 2, with a bias of 35 volts on chamber No. 1 and a 10-volt bias on chamber No. 3. Arrows indicate the biases chosen for use when running differential range spectra.

of double and triple coincidences per unit of charge collected at each absorber thickness, one obtains what is here termed an integral range spectrum. Typical integral and differential range spectra for the elastic peak from gold at 30° are shown in Fig. 4. The ratio of the area under the differential peak to the height of the integral curve below the beginning of the elastic peak gives the "range bite" of the counter. This range bite varied from 2.91 mg/cm^2 to 3.28 mg/cm^2, depending largely on the discriminator settings used, but once the discriminators were set for a run, the range bite would remain constant.

During the magnesium runs, a gold target was used for the range-bite determination because the elastic and first inelastic peaks overlapped somewhat. However, for the carbon runs, where the elastic and first inelastic peaks were well separated, the carbon elastic peak was used for the range-bite measurement.

The next step was the determination of relative differential cross sections. The counter was moved to the desired angle and the proper target inserted in the beam. For the magnesium runs, the target was placed perpendicular to the beam for cross section measurements up to 45° and at 45° to the beam for work at larger angles. At counter angles from 45° to 90° a transmission target was used, while angles beyond 90° were run with a reflection target. For the carbon runs, the CH target was always placed at 45° to the beam; the graphite target used at small angles was perpendicular to the beam. These target positions were used in order to keep the number of moves of the target to a minimum.

With the counter and target in the desired positions, a differential spectrum was run, the required data being doubles minus triples per unit charge as a function of absorber. The charge collected was adjusted to give a statistical counting error of not greater than 5% at the various peaks. Often this entailed running the various peaks at a given angle with different amounts of collected charge. The usual procedure was to map out the peak roughly by varying the absorber in steps of 2.4 mg/cm^2, and then to fill in the intervening points as thoroughly as necessary.

For both Mg and C runs, the angular distributions of the

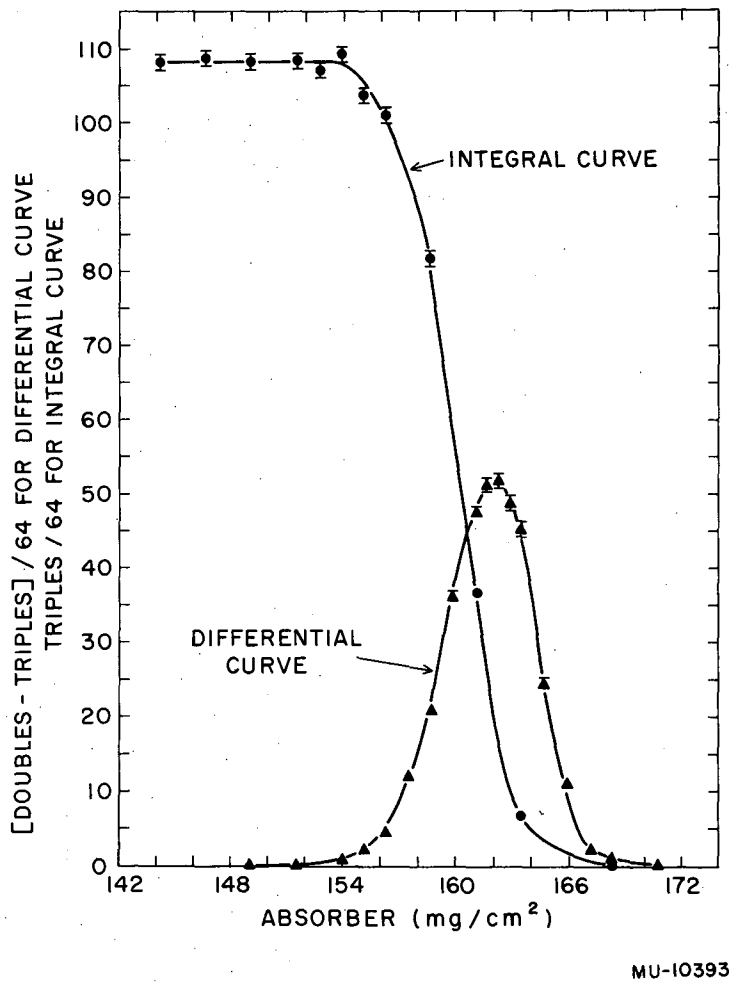

Fig. 4. Typical differential and integral curves for obtaining the "range bite" of the counter, obtained by using alpha particles on carbon with the counter at 30°.

differential cross sections were first roughly mapped out by running spectra at intervals of 10° or 15°. Then other angles were run as required to determine the detailed structure of the angular distributions. During the runs, a plot was kept of peak height per unit charge as a function of laboratory angle. Thus one could maintain a check on the results as the data were accumulated.

It was found that, to properly show the structure of the distributions, the cross section had to be found at about each degree from 7° to 15°, every 2.5° from 15° to 65°, and every 5° up to 90°. No points were taken beyond 90° on carbon, since the energy of the elastic and inelastic groups of alpha particles becomes insufficient for them to traverse the counter at angles much beyond 90°. Points were taken about every 10° from 90° out to 150° on magnesium.

It was then necessary to determine the target-out background. During the first two runs on Mg, this was done at each angle immediately after the spectrum was run. This of course involved moving the target in and out of the beam at each angle, and introduced an uncertainty into the relative-cross-section measurements because of possible nonuniformity of the target. To avoid this uncertainty, target-out background during the last Mg run and during both C runs was measured only at the end of the run. It was found that the target-out background was completely negligible at all angles with the beam levels used if the collimators were outside the chamber. During the first Mg run, the collimators were inside, and at large angles (where an intense beam was used because of the small cross sections) a considerable target-out background was found.

A somewhat different method was used to find the differential cross sections for elastic scattering from carbon. The method was essentially that used in obtaining the integral range spectrum for measuring the range bite. That is, the discriminator biases on chambers No. 1 and No. 2 were lowered and the height of the curve obtained by plotting the triple coincidences per unit charge versus absorber thickness was found at an absorber just below the beginning of the elastic peak. Any background found above the elastic peak was subtracted. This method is essentially that employed by Ellis[5] and is described by him

in detail.

To check on the proper operation and stability of the equipment during a run several steps were taken. The high voltage on the counter wires was frequently checked, using a potentiometer with which the voltages could easily be read to 1 volt. Once or twice it was found that the voltages had shifted by about 2 volts, but ordinarily they were stable throughout a run within a volt.

The timing of the gate pulses was checked by observation with the oscilloscope at least once a day. Also several times each day the counting rates were found with one of the gate pulses delayed enough so that no time overlap occurred; the accidental counts thus found were always completely negligible.

During each run a cross-section determination was repeated after two or three days. In no case did the two measurements differ significantly. Finally, in order to standardize one run against another, cross-section measurements were made at at least two of the same angles during every run using that target material. Specifically, the cross sections for elastic and inelastic scattering were found at 45° and 90° during each of the three runs using a magnesium target. During both runs in which a carbon target was bombarded, the elastic and one inelastic scattering cross section (for the 4.43-Mev level) were determined at 22.5° and at 70°.

III. REDUCTION OF DATA

Differential Cross Sections

The expression for the differential cross section per unit solid angle may be written in the form

$$\frac{d\sigma}{d\Omega} = \frac{R}{R_0 \rho \Delta\Omega} .$$

Here R is the number of scattered particles emitted into the solid angle $\Delta\Omega$ per unit of beam charge collected, R_0 is the number of beam particles that have passed through the target when a unit charge is collected, ρ is the number of target particles per square centimeter (areal density), and $\Delta\Omega$ is the solid angle within which scattered particles are counted.

For convenience in making the calculations, this expression is altered by replacing the terms on the right-hand side by constants and quantities which are directly measured in the experiment. We put R equal to AB/Q, where A is the area under the differential peak in $cm^2 \times mg/cm^2$, or mg, B is the range bite in mg/cm^2 and Q is the charge collected at each point of the peak in microcoulombs. R_0 is replaced by $1/q$, q being the charge of the alpha particle in microcoulombs, and ρ is written as $NT/M \cos \theta_T$, where N is Avogadro's number, T is the effective thickness of the target (e.g., the number of C^{12} nuclei per square centimeter of the target, when inelastic scattering from C^{12} is being considered), M is the atomic weight of the target material, and θ_T is the angle between the beam direction and the normal to the target. Also, $\Delta\Omega$ is given by S/r^2, where S is the area of the solid-angle-defining hole in front of the absorber changer in square inches and r is the distance in inches from the center of the portion of the target struck by the beam to the center of the hole of area S.

Thus the result in a form suitable for making calculations is

$$\frac{d\sigma}{d\Omega} = \left[\frac{q M r^2}{BNTS}\right] \frac{A \cos \theta_T}{Q} \quad cm^2/\text{steradian} .$$

The terms in parentheses are constants for a particular run and, in practice, θ_T had only two values, namely 0° and 45°. Thus, to calculate the differential cross sections, one first determines the values of the terms in parentheses. Then, for each laboratory angle at which data were obtained, one computes the area under the peaks of the differential range spectrum. Typical differential range spectra are shown in Fig. 5. Smooth curves were drawn through the points and the areas under the peaks were computed using Simpson's one-third rule. The charge collected in the Faraday cup for each peak was recorded, and the target angle was noted. Putting all these quantities into the above expression, one obtains the differential cross sections in the laboratory system.

A sample calculation of a cross section is given. This calculation is for the counter at a lab. angle of 22.5^o with a polystyrene target at 45° to the beam direction, the desired cross section being that for inelastic scattering leaving the C^{12} nuclei in the 4.43-Mev excited state. The charge of the alpha particle is 3.204×10^{-13} microcoulombs. The atomic weight of C^{12} is 12.004 grams per mole. The measured value of r was 12.284 inches. For this run the range bite was found to be 2.911 mg/cm^2. Avogadro's number is 6.025×10^{23} $mole^{-1}$. The measured target thickness was 6.734×10^{-3} g/cm^2; however, the polystyrene target contains one atom of hydrogen for each atom of carbon, and furthermore not all the carbon nuclei are those of C^{12}, the fractional abundance of this isotope being 0.9889. Thus T is given by (6.734×10^{-3}) (12.004) (0.9889)/(12.004 + 1.008) g/cm^2, or 6.144×10^{-3} g/cm^2. Since the hole in front of the absorber changer is round, S is given by $\pi(0.1252)^2$ in^2, 0.1252 inches being the radius. As θ_T was 45°, $\cos\theta_T$ is 0.07071. Q was measured as 0.5523 microcoulomb, and A, the area under this particular peak, was computed to be 1.344×10^4 mg. Thus, combining all these terms, we find:

$$\frac{d\sigma}{d\Omega} = 1.882 \times 10^{-26}\ cm^2/\text{steradian} = 18.82\ \frac{mb}{\text{steradian}}$$

The formula used for computing the cross sections for elastic scattering from carbon was slightly different. The integral method of

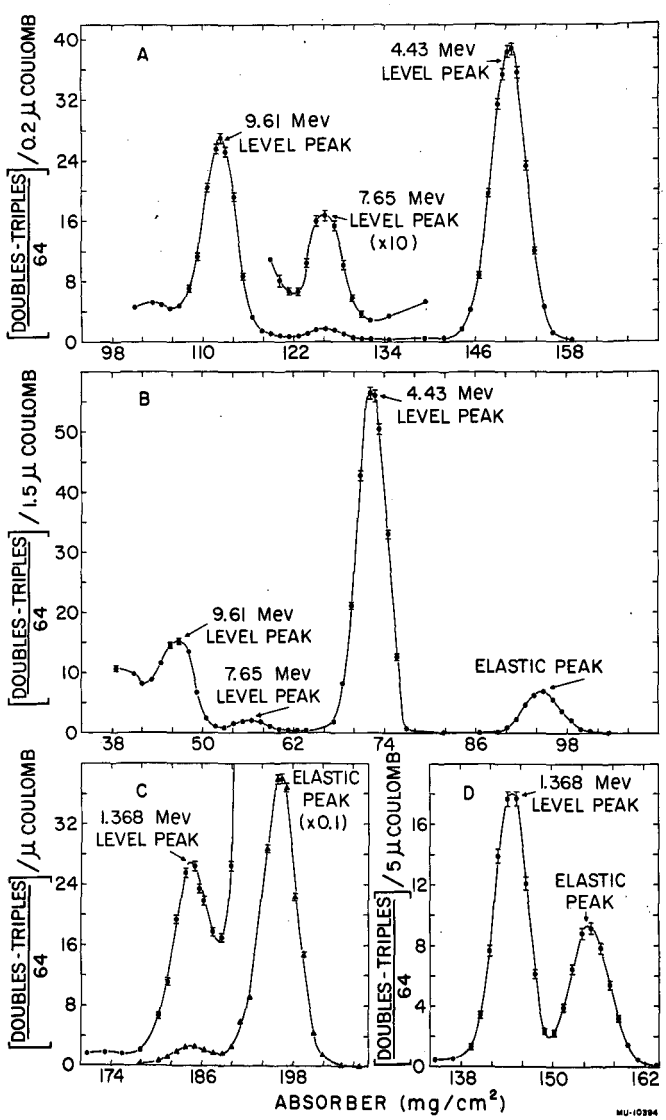

Fig. 5. Differential range spectra. A is for carbon at a counter angle of 15°. The elastic peak was integrated, so does not appear on the differential spectrum. B is for carbon at a counter angle of 60° C is for magnesium at 15°, and D is for magnesium at 56°.

counting was used, so the integral was obtained directly from the data. Thus the terms A and B are to be replaced by C, which represents the height of the integral range curve at an absorber value just below the beginning of the elastic peak.

After the differential cross sections in the laboratory system were calculated, they were converted to the center-of-mass system by use of the usual transformation formulae for cross sections and angles. The data thus obtained are the final experimental results.

Errors

The expression given above for the cross section is in the form of a product of several terms; one obtains the relative error in the cross section in the usual way by taking the square root of the sum of the squares of the individual relative errors.

Several of the factors in the cross-section formula, namely q, N, r, S, Q, and θ_T, had the same errors for all runs. M and T and their errors depended upon the target being used. B varied from run to run but had the same value and uncertainty throughout one run. The only factor whose error varied from angle to angle was A (or C, in integrating the carbon elastic peak). The terms of the formula are taken up separately, most of the discussion being devoted to the one which was the source of the largest errors.

In most cases the greatest uncertainty was that in A, the area under the peak. This area is subject to two separate sources of error. One is statistical, arising from the statistical counting errors in the points through which the curve is drawn. This error was determined in several cases by using the Simpson's rule formula and the statistical errors of the points on the curve. The error in the area was related to that of the peak point of the curve for calculating purposes. The ratio of the relative error in area to the relative error of the peak point varied slightly with angle because of the change in the width of the curve, but for convenience the same value, a conservative one, was used at all angles. This ratio was taken to be 0.48, so for the relative error in the area from this source one obtains:

$$(\delta A/A)^2 = (0.48\delta p/p)^2 = (0.48)^2 \left[(64p)^{1/2} / 64p \right]^2 = (0.48)^2 / 8p = 0.0036/p$$

where p is the number of counts at the top of the peak divided by 64 (since the scalers were set on a scale of 64). Thus, for peak heights in the range from 10 to 50 (typical of those actually used), the relative error in area because of statistical fluctuations was from 0.054 to 0.024.

The other source of uncertainty in A arose as a result of the closeness of some of the peaks to one another. For magnesium, the elastic and inelastic peaks overlapped somewhat at all angles. And with carbon, the 7.65-Mev-level peak partially overlapped the 9.61-Mev peak at all angles; it also merged somewhat with the 4.43-Mev-level peak at angles greater than about 60°. Furthermore, the 9.61-Mev-level peaks were partially overlapped on the low-energy side by peaks from higher levels. At small angles, where the elastic peak rapidly becomes very large, the low-energy "tail" of the elastic peaks extended into the 4.43-Mev-level peak of carbon and into the inelastic magnesium peak. All this overlapping produced an uncertainty in the position of the curves, particularly near the base line. Another factor that made the area under the 7.65- and 9.61-Mev carbon peaks uncertain was the possible presence of a continuum alpha-particle background arising from the decay of carbon nuclei, excited by 7.37 Mev or more, into an alpha particle and Be^{8}. In cases where overlapping or a possible continuum background was present, three curves were drawn, one giving the estimated "best" value for the area, one giving the maximum reasonable value, and the third giving the estimated minimum. The possible errors thus estimated were by far the largest source of uncertainty in the cross sections for scattering from the 7.65- and 9.61-Mev excited states of carbon, the relative error in area being as high as one-fourth or even one-third at some angles. The large possible continuum background accounts for the fact that for these levels the cross section may in many cases be much lower, but not very much higher, than the estimated "best" value. At small angles the uncertainty in area because of overlapping also produced large uncertainties in the areas of the 4.43-Mev carbon peaks and in the inelastic magnesium peaks. At large angles, the elastic-scattering cross section for magnesium becomes very small compared to that for

scattering to the first inelastic level, and thus the areas of the elastic peaks cannot be measured very accurately. At most angles, however, there was very little uncertainty (other than statistical) involved in drawing the curves for the elastic peaks, the inelastic peaks of magnesium, and those of the 4.43-Mev level of carbon, and this source of error thus became comparable to or smaller than the various others.

Several other quantities were sources of significant uncertainty in the cross sections.

The largest of these uncertainties was found to be in the range bite of the counter, B. The range bite is composed of two factors, namely the area under an elastic peak run differentially, and the height of the integral curve below the elastic peak. Both factors have statistical errors and the resulting error in B was found to have the value (for a typical run),

$$\delta B/B = 0.040/2.911 = 0.0103.$$

The aperture that defined the solid angle was a round hole. Its radius was measured by use of a travelling microscope. Since the radius appears squared in the cross-section formula, the relative error in S is given by

$$\delta S/S = 2\,\delta R/R = (2)\,(0.0005)/0.1252 = 0.00799.$$

The charge collected, Q, was the product of three factors: Q = (C) (SF) (D), where C is the capacity of the condenser being charged, SF is the scale factor used on the Speedomax recorder (in volts), and D is the number of "dumps", or the number of times the charge (C)x (SF) is collected before the scalers are stopped. The values of the capacitors used were carefully determined by comparing them with a standard whose capacity was known to 0.1%. The scale factors were measured by observing the recorder readings when an accurately known voltage was placed across the recorder input. Both C and SF were measured several times, and were found to remain quite constant. The fractional errors in the various capacities and scale factors were very nearly the same, so for convenience a single value for the uncertainty in Q was adopted. This value was taken to be $\delta Q/Q = 0.00542$.

The correspondence between the actual target angle and that indicated on the control panel dial was carefully measured by visual

observations with a telescope, with the target both parallel to and perpendicular to the beam direction. In each case the difference between the angle actually observed and that indicated on the dial was about 0.1°. In practice the target was often used at 45° to the beam, so a conservative estimate of 0.25° as the maximum difference between the true target angle and the indicated target angle was made. This estimated error in target angle gives

$$\delta \cos s_T / \cos \theta_T = 0.0031/0.07011 = 0.00438.$$

The distance from the center of the target to the aperture defining the solid angle was measured, and a correction was applied because the beam did not pass precisely through the center of the target. The estimated uncertainty of the measurements gave the result,

$$2\,\delta r/r = (2)\ 0.025/12.284 = 0.00407.$$

The target thickness was found in the usual fashion by measuring the area of the target and weighing it. After the runs during which the polystyrene and magnesium targets were used, the center portions of the targets (through which the beam passed) were cut out and their thicknesses were determined. In neither case did the result disagree with that obtained from use of the whole target by more than 0.2%; thus the targets were evidently quite uniform. For the polystyrene target the probable error in T resulting from the errors in the weighing and measuring processes was found to be $\delta T/T = 0.0085/6.7342 = 0.00126$.

The probable errors in the constants appearing in the cross-section formula, namely M, N, and q, are completely negligible compared with the other sources of error.

The calculation of cross sections when the graphite target was used involved another source of error. This arose from the fact that the thickness of the graphite target was not measured directly. It was measured indirectly by comparing the areas under two peaks run with the graphite target with the areas under these same two peaks when the polystyrene target was bombarded. The graphite target was used at laboratory angles smaller than 15°, where the alpha-particle peak from (α, p) scattering masked some of the inelastic peaks. Actually the graphite target itself was contaminated with hydrogen enough to prevent

the measurement of the 4.43-Mev level peak at 9°, the 7.65-Mev peak at 11° and 12°, and the 9.61-Mev peak at 13°. Although the graphite target was not expected to be of very uniform thickness, it was used in only one position, and its indirectly measured thickness was therefore the same for all angles at which it was employed.

The measurements of the cross sections for elastic scattering by carbon involved only a statistical error in the height of the integral range curve, rather than the previously discussed errors in A and B. At several angles the cross sections were found by using both the differential and the integral methods; in all cases the results agreed within the estimated uncertainties, indicating that the range bite remained quite constant during a run.

A sample calculation of the uncertainty in a cross section is given here; the cross section concerned is that whose magnitude has previously been computed. All the numerical values that have been given above for the errors in the various factors of the cross section formula are applicable (e.g., the error in target thickness was given for the polystyrene target). Thus, combining the squares of all the uncertainties whose magnitudes have been listed, and putting in the expressions for the errors in A, we have

$$\frac{\delta\left(\frac{d\sigma}{d\Omega}\right)}{\frac{d\sigma}{d\Omega}} = \pm \sqrt{\left(0.000319 + \frac{.0036}{p}\left(\frac{e}{A}\right)^{2}\right)}^{\frac{1}{2}} .$$

Here e is the estimated uncertainty in the area under the peak because of overlapping or background. The first factor on the right-hand side contains the errors in all factors except A, and indicates that the combined uncertainty in these factors was about 1.8 % for this run. This is a typical value; it was a little higher when the graphite target was used, for the reason noted above, and somewhat lower when the integration method was used, as also explained above.

For this particular case, the peak height was 32.7. The area under the peak was estimated to be no greater than that under the "best" curve (except for statistical considerations which are taken into account

by the second factor on the right). However, it was estimated that the area might be as much as 2.92 mg less than the "best" value of 105.0. Thus for the relative error we obtain

$$\frac{\delta\left(\frac{d\sigma}{d\Omega}\right)}{\frac{d\sigma}{d\Omega}} = \begin{matrix} +\left(0.000319 + \frac{0.0036}{32.7} + 0\right)^{\frac{1}{2}} \\ -\left(0.000319 + \frac{0.0036}{32.7} + \left(\frac{2.92}{105}\right)^2\right)^{\frac{1}{2}} \end{matrix} .$$

The cross section, including the uncertainty, is then given by

$$\frac{d\sigma}{d\Omega} = 18.82 \begin{matrix} +0.39 \\ -0.65 \end{matrix} \text{ mb/steradian.}$$

There were two other sources of error whose magnitudes could not be well estimated. The first of these arose from the fact that the beam energy changed somewhat as various cyclotron parameters, particularly the oscillator power, were varied. In practice this energy change appeared largely as an increase as the oscillator power was increased. Since the beam intensity, and therefore the oscillator power, had to be varied somewhat with counter angle to obtain reasonable counting rates, these energy changes could not be avoided. Thus measurements were made at small angles, where the cross sections were large, using a smaller beam energy than that used when the cross sections were small. The maximum observed beam energy difference between the smallest and largest counter angles were about 0.5 Mev, or 1%, the average energy being about 48 Mev.

Another source of uncertainty in the angular distributions from magnesium was the fact that naturally occurring magnesium was used for the target. The normal abundance of Mg^{24} is 78.60%, with 10.11% Mg^{25} and 11.29% Mg^{26} also present. Thus the observed elastic angular distribution, which included alpha particles elastically scattered by all three isotopes, was really a weighted average. And the inelastic alpha-particle peaks from the 1.368 Mev level of Mg^{24} were contaminated with particles inelastically scattered from the 0.98-, the 1.61-, and the 1.96-Mev levels in Mg^{25}, and from the 1.83-Mev level in Mg^{26}. These various contaminants could badly distort the angular distribution of the

desired alpha particles, but there was no way of subtracting them. The inelastic alpha-particle peaks exhibited "bumps", which may have been caused by inelastic alpha particles from levels in the other isotopes, at only about three angles.

For carbon this source of error is also present, but in a relatively negligible amount, since the abundance of C^{12} is 98.892%.

IV. RESULTS AND CONCLUSIONS

Elastically Scattered Alpha Particles

Carbon target

The experimental differential cross sections for the elastic scattering of 48 Mev alpha particles from carbon are listed in Table I. The ratio of the observed cross section to the Rutherford cross section is also given at each angle. The Rutherford cross section is taken to be

$$\frac{d\sigma}{d\Omega_R} = \left(\frac{ZZ'e^2}{4E}\right)^2 \frac{1}{\sin^4 \frac{\theta_C}{2}}$$

Here $Z'e$ is the charge of the alpha particle, Ze is the charge of the target nucleus, E is the bombarding energy in the center-of-mass system, and θ_C is the center-of-mass scattering angle. The absolute differential cross section and the Rutherford cross section have been plotted as functions of the center-of-mass scattering angle in Fig. 6.

As mentioned in the introduction, Blair[3] has formulated a semi-classical model with which attempts have been made to fit observed angular distributions of 22- and 48-Mev alpha particles elastically scattered from Ag, Au, and Pb. However, the model would be considerably less applicable to scattering from light elements than from heavy ones, since $\lambda\!\!\!^{-}/R$ is smaller for the smaller radii and therefore the picture is less nearly classical.

Various optical models of the nucleus have been used in trying to fit observed angular distributions of elastically scattered protons. Melkanoff, Nodvik, Saxon, and Woods,[1] for example, using such a model, have obtained good fits out to about 150° for elastic scattering of 17-Mev protons from several elements. A four-parameter proton-nuclear interaction of the following form is assumed:

$$-V_N(r) = \frac{V + iW}{1 + \exp\left(\frac{r - R_0}{a}\right)}$$

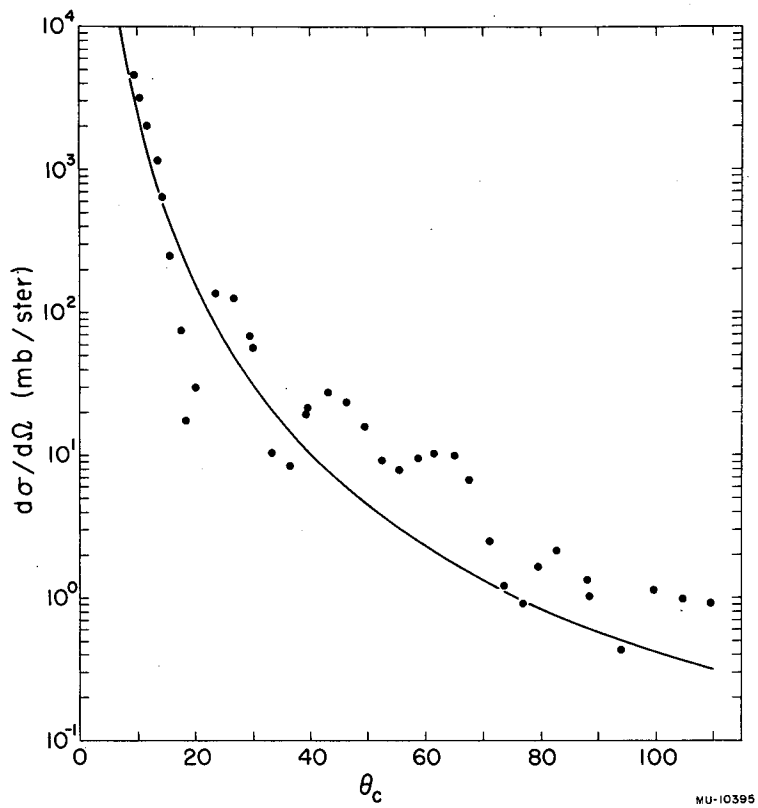

Fig. 6. Angular distribution of the differential cross section (c.m.) for elastic scattering of 48-Mev (lab) alpha particles from carbon. The solid curve indicates the Rutherford cross section.

$$V_C(r) = \begin{cases} \dfrac{Ze^2}{2R_0}\left(3 - \dfrac{r^2}{R_0^2}\right) ; & r \leq R_0 \\ \dfrac{Ze^2}{r} , & r \geq R_0 \end{cases} .$$

V and W are the real and imaginary parts of the nuclear potential, which has the shape of a rounded square well. R_0 is the "radius" of the well, and a is the rounding or "diffuseness" parameter. $V_C(r)$ is the Coulomb potential for a proton and a nucleus of charge Ze, this charge being uniformly distributed over a sphere of radius R_0.

By use of this form of interaction, the complex phase shifts and hence the angular distributions are found as functions of the four parameters, the lengthy calculations being performed with the aid of a computer. By systematically varying the four parameters, one finds the values which give the best fit to experimental results. The "best" parameters were found to be quite consistent for the various elements, even though all four were varied independently for each element in the calculations. Values that give reasonable fits over the whole periodic table for elastic scattering of 17-Mev protons are:

$$V = 45.5 \pm 1.5 \text{ Mev}; \; W = 8.5 \pm 0.5\text{-Mev};$$
$$R_0/A^{1/3} = 1.33 \pm 0.03 \times 10^{-13} \text{ cm.};$$

and

$$a = 0.49 \pm 0.02 \times 10^{-13} \text{ cm.}$$

Attempts could be made to fit angular distributions of elastically scattered alpha particles by using an optical model of the above or similar nature, although no results of such attempts have been published. However, it is planned to make arrangements to have the present data on elastic scattering analyzed by use of optical-model methods.

Since such arrangements will be made, and since both Blair model and optical model calculations are quite lengthy and can best be done with a computer, no extended attempts were made to analyze the elastic scattering data. However, a greatly simplified version of the optical model calculations outlined above was used to see if any

reasonable results could be obtained. A complex square-well nuclear potential of the form $-(V + iW)$ was assumed, the radius of the well being R_0. And a simple point-charge Coulomb potential of the form $\frac{ZZ'e^2}{r}$ was also assumed. Then, using these potentials and the Born approximation,[14] the differential cross section for elastic scattering of alphas as a function of V, W and R_0 was found. The result, with numerical values appropriate to scattering of 48-Mev alpha particles from carbon inserted, is

$$\frac{d\sigma}{d\Omega} = \frac{9.96 \times 10^{-3} \; R_0^{\,4}(V^2 + W^2)}{\sin^2 \theta/2} \left[j_1(kR_0)\right]^2 + \frac{0.144}{\sin^4 \theta/2}$$

$$- \frac{7.57 \times 10^{-2} \; R_0^{\,2} \; V j_1(kR_0)}{\sin^3 \theta/2} \quad \text{mb/steradian.}$$

Here V and W are in Mev, θ is the center-of-mass scattering angle, and j_1 is the spherical Bessel function of order one. K is given by $2kR_0 \sin \theta/2$, where k is the wave number corresponding to the center-of-mass energy of the bombarding alpha particle in units of 10^{13} cm.$^{-1}$, and R_0 is in units of 10^{-13} cm.

From the above expression, it can be seen that the ratio of the cross section to the Rutherford cross section (second term), becomes unity when $j_1(KR_0)$ is zero, or when the first term is equal to the third term and has the same sign. From the plot of Fig. 6, this ratio becomes unity for the first time at 14.5° and for the second time at 22.3°. Since the first zero of $j_1(x)$, (after $x = 0$) occurs when x is 4.49, one can find R_0 from the equation

$$R_0 = \frac{4.49}{2k \sin \theta/2} = \frac{0.988}{\sin \theta/2} ,$$

when the value of k is inserted. Putting $\theta = 14.5^\circ$, one obtains $R_0 = 7.03$ and, putting $\theta = 22.3^\circ$, one finds $R_0 = 5.11$. The latter is a much more reasonable value for carbon; it corresponds to $r_0 = 1.62$ in the usual equation for a nuclear radius, $r = r_0 A^{\frac{1}{3}} \times 10^{-13}$,

if one uses 1.4×10^{-13} as the alpha-particle radius.

Inserting $R_0 = 5.11$, therefore, in the formula for the differential cross section, one can attempt to fit the experimental curve by adopting suitable values of V and W. This was done, but it was found impossible to fit an extended portion of the observed distribution with one set of values for V and W. The best that could be done was to obtain a rough fit over a region of the curve from one maximum or minimum to the next; at smaller and larger angles the calculated cross section rapidly diverged from that observed.

This is not surprising, however. First of all, the criterion for the validity of the Born approximation does not hold for a reasonable magnitude of the nuclear potential for the experimental conditions. Secondly, as pointed out in Reference 1, an optical model using a simple square-well potential does not yield good fits to experimental results.

A simple procedure has been applied to obtain estimates of the interaction radius from angular distributions of alpha particles elastically scattered from aluminum at 19 and 40 Mev.[6, 7] One assumes that, for adjacent maxima or minima in the angular distribution, one can put $2kR_0 \ \Delta(\sin \theta/2) = \pi$. Here k is the wave number associated with the center-of-mass bombarding energy, and θ is the angle at which a maximum or minimum occurs. Inserting the value of k and the values of $\sin \theta/2$ for adjacent maxima or minima gives one R_0. This is thought of as being the sum of the radii of the nucleus and the alpha particle. This procedure is approximately valid if elastic alpha scattering may be treated analgously to Fraunhofer diffraction from an opaque disk. In that case one obtains an angular distribution proportional to $\left[J_1(KR_0)\right]^2$, where J_1 is the ordinary Bessel function of first order. Since the zeros and maxima of this function are separated by approximately π, the relation used is obtained. Also, as can be seen from the crude formula derived here for the cross section for elastic scattering, that cross section will be nearly proportional to $\left[j_1(KR_0)\right]^2$ if the nuclear scattering is much larger than the Coulomb scattering. Thus, since j_1 also has its adjacent maxima and minima separated by a number close to π, the relationship employed would

be valid for that case.

If applied to the observed distribution of elastic alphas from carbon, this formula gives an average value for R_0 of 5.1, which agrees very well with that obtained previously.

Magnesium target

The experimental differential cross sections for the elastic scattering of 48-Mev alpha particles from magnesium are listed in Table II. The ratio of the observed cross section to the Rutherford cross section is also given for each angle at which observations were made. The observed differential cross sections together with the Rutherford cross sections are shown graphically in Fig. 7.

The first procedure followed with the carbon data could not be applied in the case of magnesium. A formula was calculated for the differential cross section, using the same type of potential as for carbon and again employing the Born approximation. The result was of the same form as for carbon, but with the constants changed. Therefore the formula still indicated that the ratio to Rutherford should be unity when j_1 is zero. However, the experimental ratio to Rutherford is below 1 at all angles, so no attempt could be made to fit the formula to the observed cross section. As stated previously, failure to obtain a reasonable result is not surprising because of the potential assumed and in view of the fact that the Born approximation is known to be unsuitable.

The second procedure, namely putting $2kR_0 \Delta(\sin \theta/2) = \pi$, was used. It gave an average value of 6.3 for R_0. If one takes 1.4×10^{-13} as the radius of the alpha particle, this leads to a value of 1.7 for r_0 in the formula $r = r_0 (A)^{\frac{1}{3}} \times 10^{-13}$.

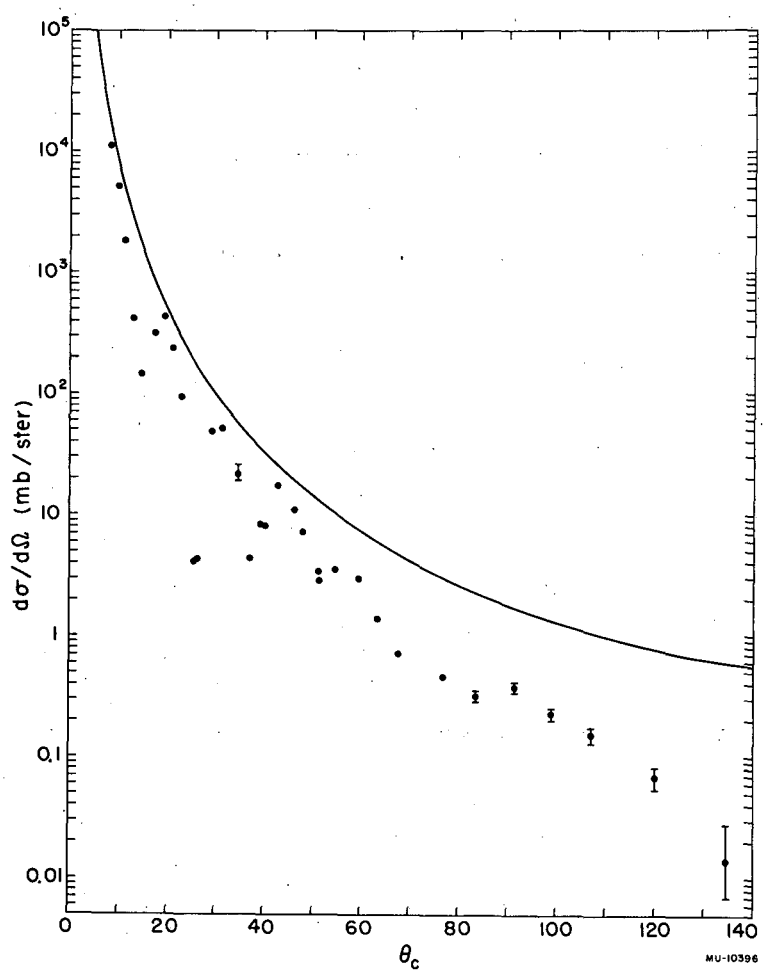

Fig. 7. Angular distribution of the differential cross section (c.m.) for elastic scattering of 48-Mev (lab) alpha particles from magnesium. The solid curve indicates the Rutherford cross section.

Inelastically Scattered Alpha Particles

General Considerations

The experimental cross sections for the inelastic scattering of 48-Mev alpha particles from the 4.43-, the 7.65-, and the 9.61-Mev levels of carbon[12] and from the 1.368-Mev level of magnesium[24] are listed in Tables III to VI.

At laboratory angles of 14° and 47.5° a search was made for inelastic groups of alpha particles from levels in carbon in the range from 14 to 21 Mev above the ground state. The first level in carbon with isotopic spin unity is at an excitation of 15.09 Mev;[15] conservation of isotopic spin forbids excitation of this level with alpha particles. In accordance with this conservation principle, no trace of an inelastic alpha group from a level near 15 Mev was found at either angle. Strauch and Titus,[16] bombarding carbon with 96-Mev protons, observed a fairly large inelastic peak corresponding to an excitation of 20.0 ± 1.0 Mev, observations being made at a laboratory angle of 40°. No such group was observed at either angle with alpha-particle bombardment.

As stated in the introduction, compound-nucleus theory predicts angular distributions of inelastically scattered particles which are symmetric about 90° in the center-of-mass system. The observed differential cross sections at angles greater than 90° are very small for magnesium, which indicates, considering the symmetry, that the large cross sections observed in the forward hemisphere are largely due to a process other than compound nucleus formation. Although observations were not made on carbon at angles much greater than 90° in the center-of-mass system, one would expect a similar situation to prevail; namely, the cross sections at large angles would be very small compared with those observed at small angles. Rough computations of the maximum possible cross sections for inelastic alpha-particle scattering in which a compound nucleus is formed[8] indicate that these cross sections are negligible in comparison with those observed.

The other general type of theory that has been used to explain and predict angular distributions is based on surface or direct interactions. No such theory has been applied directly to inelastic alpha-

particle scattering. However, in at least a crude way, the same physical picture that leads to the Austern, Butler, and McManus theory[11] (later abbreviated as the ABM theory) for angular distributions of inelastically scattered protons may be applied to inelastic alpha-particle scattering. Briefly, one thinks in the ABM theory of a proton colliding with a nucleon near the nuclear surface, imparting some energy to it, thereby exciting the nucleus, and then going on. The authors state that, because of the approximations used, it is not to be expected that the theory will accurately predict angular distributions. However, it may be possible to fit observed results at fairly small angles, in which case one may obtain some information about the spins and parities of the excited nuclear states. The results of the theory for protons are briefly given, first, and certain differences to be expected for the case of inelastic alpha-particle scattering are presented.

The ABM theory leads to angular distributions of inelastically scattered protons of the form

$$\frac{d\sigma}{d\Omega} \propto \sum_{\ell} \left[a_{\ell}\, j_{\ell}(GR_0) \right]^2 ,$$

Here a_ℓ is a coefficient depending only on ℓ, j_ℓ is the spherical Bessel function of order ℓ, R_0 is the nuclear radius, and G is the magnitude of the vector difference between the wave numbers of the incoming and outgoing protons, i.e:

$$G = \left| \vec{k}_{in} - \vec{k}_{out} \right| = \left[k_{in}^2 + k_{out}^2 - 2\, k_{in}\, k_{out} \cos \theta_C \right]^{\frac{1}{2}} .$$

Here θ_C is the scattering angle in the center-of-mass system, and ℓ is restricted to certain values given by

$$J_i + J_f + 1 \geq \ell \geq \left| \vec{J}_i + \vec{J}_f + \vec{1} \right|_{min.}$$

Here J_i is the spin of the nucleus in its initial (ground) state and J_f is the spin in the final (excited) state; ℓ is further restricted to only even or odd values according to whether or not there is a change of parity between the initial and final states of the target nucleus. If one puts $\Delta J = \left| \vec{J}_i - \vec{J}_f \right|$, then ΔJ is $\ell \pm 1$ or 0, the ± 1 allowing for

possible spin flips of the proton. The position of the first maximum in the angular distribution gives ℓ_{min}, where

$$\ell_{min} \geq \left| \vec{J}_i + \vec{J}_f + \vec{1} \right|_{min} .$$

Thus a peak directly forward (ℓ_{min} = zero) would indicate $\Delta J = 0$ or 1 with no parity change. No peak directly forward ($\ell_{min} \geq 1$) would mean either $\Delta J \geq 0$ with a parity change or $\Delta J \geq 2$ with no parity change.

To apply this theory to alpha particles, without attempting any sort of detailed justification, one may think of an alpha particle colliding with a surface nucleon, imparting to it energy and angular momentum, and going on. In fact, it would even seem reasonable for the observed angular distributions of inelastically scattered alpha particles to be more in accord with the predictions of the ABM theory than is the case for protons. Alpha particles in this energy range have a very short mean free path in nuclear matter, and therefore one would expect direct interactions to occur only for alpha particles that strike very near the outer edge of the nucleus. For protons, however, which have a longer mean free path, it may happen that some direct interactions take place for protons striking the nucleus well within the outer edge. The ABM theory takes into account only those direct interactions which are also surface interactions; thus it accounts for essentially all direct interactions of alpha particles, but it may not do as well for protons.

The alpha particle has zero spin, and therefore one would expect some changes in the selection rules. First of all, since the alpha particle has no spin to flip, one puts $\Delta J = \ell$ only. The selection rule for ℓ assumes the form

$$J_i + J_f \geq \ell \geq \left| \vec{J}_i + \vec{J}_f \right|_{min} .$$

The same parity considerations would apply. For carbon and magnesium, both having a ground-state spin of zero, only one ℓ value would be allowed, namely $\ell = J_f$. Thus an unambiguous determination of the spin of the excited states of these nuclei could be made--providing the observed distribution is in accord with the theory. The results of the ABM theory in this form were compared with the observed angular distributions.

Inelastic scattering from carbon

4.43-Mev level

The ground state of carbon-12 is known to be a (0, +) state,[15] i.e. its spin is zero and its parity is even. The first excited state at 4.43 Mev is a (2, +)[15] state. Therefore we have $\Delta J = 2$ and no change in parity. From the selection rules of the ABM theory as modified for inelastic alpha scattering, we then must have $\ell = 2$ only; the angular distribution should be proportional to $\left[j_2(GR_0) \right]^2$. Figure 8 shows the experimental angular distribution and a plot of j_2^2 normalized to fit the height of the observed peak at 25° and with R_0 chosen to give a best fit. The value used for R_0 was 5.56×10^{-13} cm. This corresponds to $r_0 = 1.80$ in the usual formula for the nuclear radius ($r = r_0 A^{1/3} \times 10^{-13}$ cm) if one assumes a value of 1.4×10^{-13} cm. for the alpha-particle radius. The fit may be termed reasonable for small angles, but by no means excellent. Unfortunately the errors become large at the most forward angles because the elastic peak runs into that of the 4.43-Mev level at these angles.

If the spin and parity of the excited state were not known, one would attempt to fit the observed distribution at forward angles using spherical Bessel functions of various orders. The "goodness of fit" of the various j_ℓ's was determined for this case to determine how useful a tool inelastic alpha-particle scattering might be to determine spins and parities of levels for which these constants are not known. Best fits were obtained with j_1^2 for $r_0 = 1.35$ and with j_3^2 for $r_0 = 2.4$. Higher values of ℓ would give even higher values of r_0. Neither j_1^2 nor j_3^2 fits the general shape of the observed distribution as well as j_2^2, however. The r_0 for a best fit with the j_2^2 curve is also the most reasonable, (since direct interaction theories usually result in a value for r_0 slightly larger than that found using other methods for determining nuclear radii). Choosing a somewhat larger value for the alpha-particle radius would of course result in correspondingly smaller values for r_0. Thus, both from the general fitting of the experimental curve and from the magnitude of r_0 found, one can say that the best-fitting theoretical angular distribution is in agreement with the known spin and parity of this state.

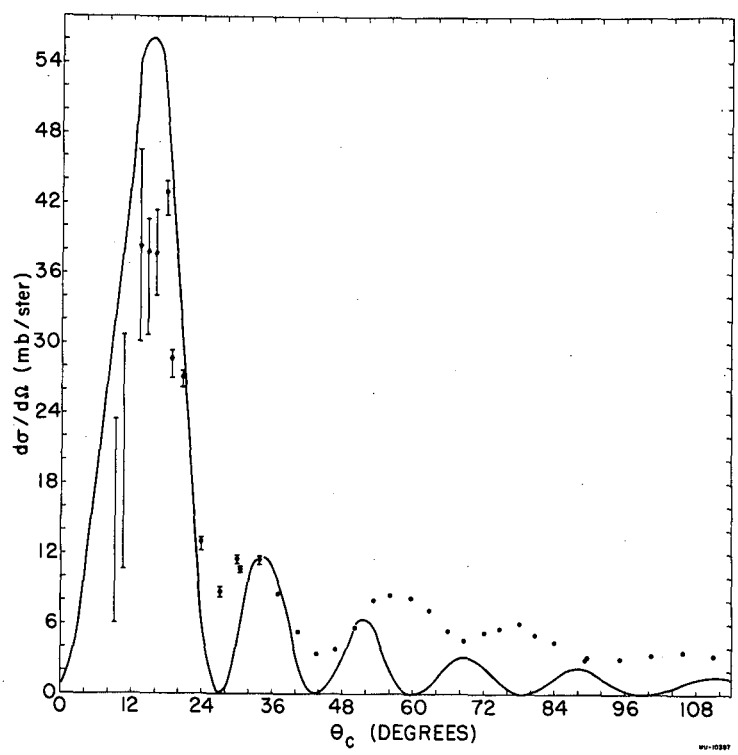

Fig. 8. Angular distribution of the differential cross section (c.m.) for the reaction C^{12} (α, α') C^{12*}, Q = -4.43 Mev. The solid curve is $[j_2(GR_0)]^2$ for $R_0 = 5.56 \times 10^{-13}$ cm.

Angular distributions of inelastic protons from this level of carbon have been observed most recently by Fischer[12] at 10 Mev, by Conzett at 12 Mev,[17] and by Hecht[18] at 31 Mev. Fischer did not attempt to fit the ABM theoretical curve; his observed angular distribution was nearly symmetrical about 90°, with peaks at about 35° and 135°, the forward peak being slightly higher. Conzett's results have not yet been analyzed; Hecht found no agreement with a j_2^2 distribution and concluded the theory in its present form is inadequate to explain his results.

Freemantle, Gibson, and Rotblat[19] have observed the angular distribution of inelastic deuterons from the 4.43-Mev level of carbon at an energy of 19 Mev. Their results however, have not been compared with theoretical predictions. The theory developed by Huby and Newns[10] to explain inelastic scattering of deuterons gives angular distributions similar to those of the ABM theory, and could presumably be used for an analysis.

7.65-Mev level

The angular distribution of alphas inelastically scattered from carbon leaving the residual carbon nucleus in the 7.65-Mev excited state, is shown in Fig. 9. The uncertainties are quite large, one reason being that the cross sections for scattering from this level are considerably smaller than those for scattering from the 4.43- or the 9.61-Mev levels. Another source of uncertainty is the presence of a continuum background beginning at 7.37-Mev excitation; carbon-12 excited by that amount or more can break up into Be^8 and an alpha particle. The magnitude of this continuum could not be well determined, since the 7.65-Mev and the 9.61-Mev peaks are too close together for the counting rate to fall to the continuum between the peaks. However, the angular distribution of this background would not be expected to be a rapidly changing function of angle. The "best" cross sections are for essentially no continuum, and the smallest indicated values are for the estimated maximum possible continuum. Therefore any such background would shift each point down by roughly the same amount; it would change the height of the whole curve, but not its shape.

The 7.65-Mev level is known to be (0, +),[15] so the angular

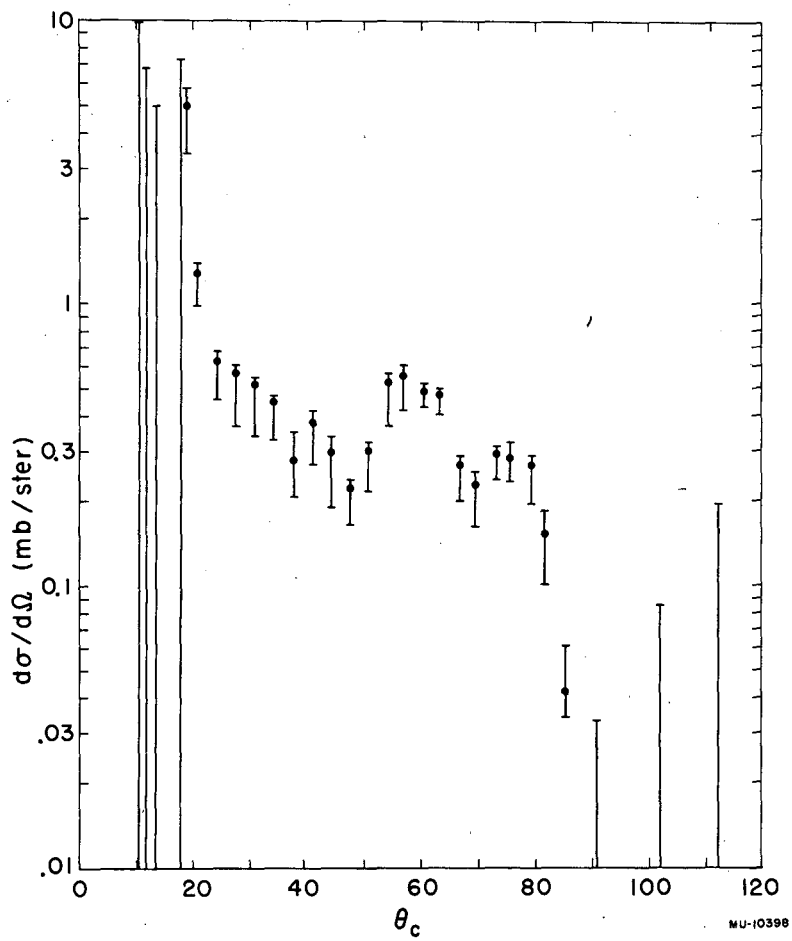

Fig. 9. Angular distribution of the differential cross section (c.m.) for the reaction $C^{12}(\alpha,\alpha')\,C^{12*}$, Q = - 7.65 Mev.

distribution should be proportional to $\left[j_0(GR_0)\right]^2$, according to the ABM theory. However, to fit the first minimum of the observed distribution, R_0 must be chosen to be 1.8×10^{-13} cm, giving an r_0 of 0.8 even if no allowance is made for the alpha-particle radius. If one assumes a first minimum at 23°, where the slope of the angular distribution decreases, one finds $R_0 = 11.9 \times 10^{-13}$ cm, which is too large. Thus the theoretical distribution does not fit that observed. One possible reason may be that the ABM theory is expected to fit only distributions in which the excited state of the nucleus arises from simple single-particle excitation. This may not hold true for the 7.65-Mev state of carbon.

Inelastic particles leaving carbon in this excited state have been searched for by Hecht,[18] bombarding with 31-Mev protons, and by Freemantle, Gibson, and Rotblat,[19] using 19-Mev deuteron bombardment. No such inelastic group was observed, no doubt because of the relatively low cross sections. Conzett,[17] using 12-Mev protons, observed inelastic protons from this level at one angle, the cross section being considerably lower than that for inelastically scattering protons from the 4.43-Mev level at that angle. Alpha particles inelastically scattered from the 7.65-Mev level have previously been observed by Rasmussen, Miller, Carmichael, and Sampson[20] at several angles, 22-Mev alpha particles being used for bombardment. It is not known whether any cross sections were measured.

9.61-Mev level

The angular distribution of alpha particles scattered from the third excited level of carbon-12, at 9.61 Mev excitation, is shown in Fig. 10. Again the uncertainties are large because of the possible continuum background. The spin and parity of this level are not known. Obviously no single j_ℓ^2 curve will fit the observed distribution. The theory is evidently inadequate to explain the observed results.

The angular distribution of inelastic protons from this level has been measured by Hecht,[18] using 31-Mev protons. The general shape of his observed distribution at forward angles is in agreement with a j_1^2 curve. Application of the selection rules gives 0, 1, or 2 for the

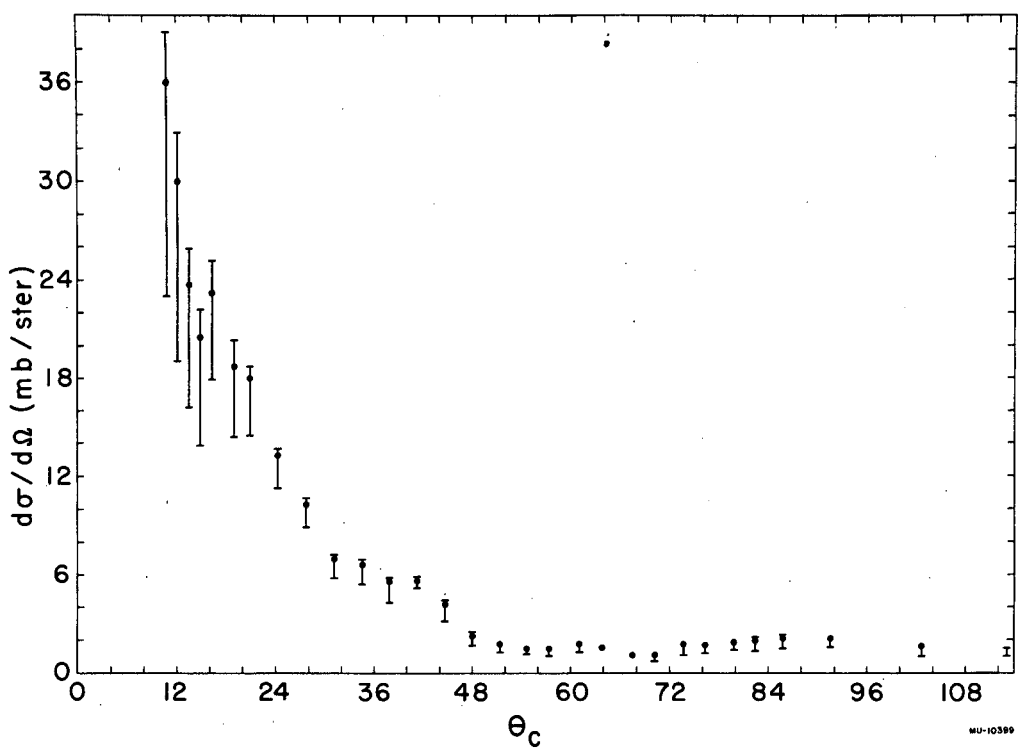

Fig. 10. Angular distribution of the differential cross section (c. m.) for the reaction $C^{12}(\alpha, \alpha')C^{12*}$, Q = - 9.61 Mev.

spin of the excited state, while its parity must be odd. The reason for the disagreement between Hecht's results and those reported here is not known; it may be, as Hecht points out, that the fit of his results with j_1^2 is merely fortuitous.

Freemantle, Gibson, and Rotblat[19] have observed inelastic deuteron scattering from this level, again using 19-Mev deuterons. Their observed curve is similar in general shape to those observed with protons and alpha particles (i.e., it is peaked near the forward direction); no analysis was made, however.

Inelastic scattering from magnesium

The angular distribution of 48-Mev alpha particles inelastically scattered from the 1.368-Mev level of Mg^{24} is shown in Fig. 11. The ground state of Mg^{24} is a $(0, +)$[15] state, and the 1.368-Mev level is known to be $(2, +)$.[15] Therefore the angular distribution should be given by j_2^2. The theoretical curve for $R_0 = 6.60 \times 10^{-13}$ cm corresponding to $r_0 = 1.8$, and normalized to fit the height of the 25° peak, is also shown. The fit is quite good at small angles--much better than for the 4.43-Mev level of carbon. No other j_ℓ^2 will give a reasonable fit to the experimental curve except j_1^2; the value of R_0 found from the j_1^2 curve is 5.2×10^{-13} cm, corresponding to $r_0 = 1.3$. However, the fit is not as good as with the j_2^2 curve, and the radius for the best fit is somewhat small. Therefore one could, assuming the validity of the ABM theory and its applicability to inelastic alpha-particle scattering, determine the spin and parity of the 1.368-Mev level of Mg^{24} from the observed angular distribution.

Angular distributions of protons inelastically scattered from this level have been measured by Fischer[12] and by Conzett,[17] using 10- and 12-Mev protons respectively. Fischer concluded that his results are in accord with a j_2^2 distribution if one subtracts the contribution made by scattering processes in which a compound nucleus is first formed. Conzett's data have not yet been analyzed, although preliminary examination indicates that his data will not fit a j_2^2 curve.

The distribution of 7.5-Mev deuterons inelastically scattered from the 1.368-Mev level has been observed by Holt and Young.[21] Their curve is apparently of the direct interaction type, but no comparison

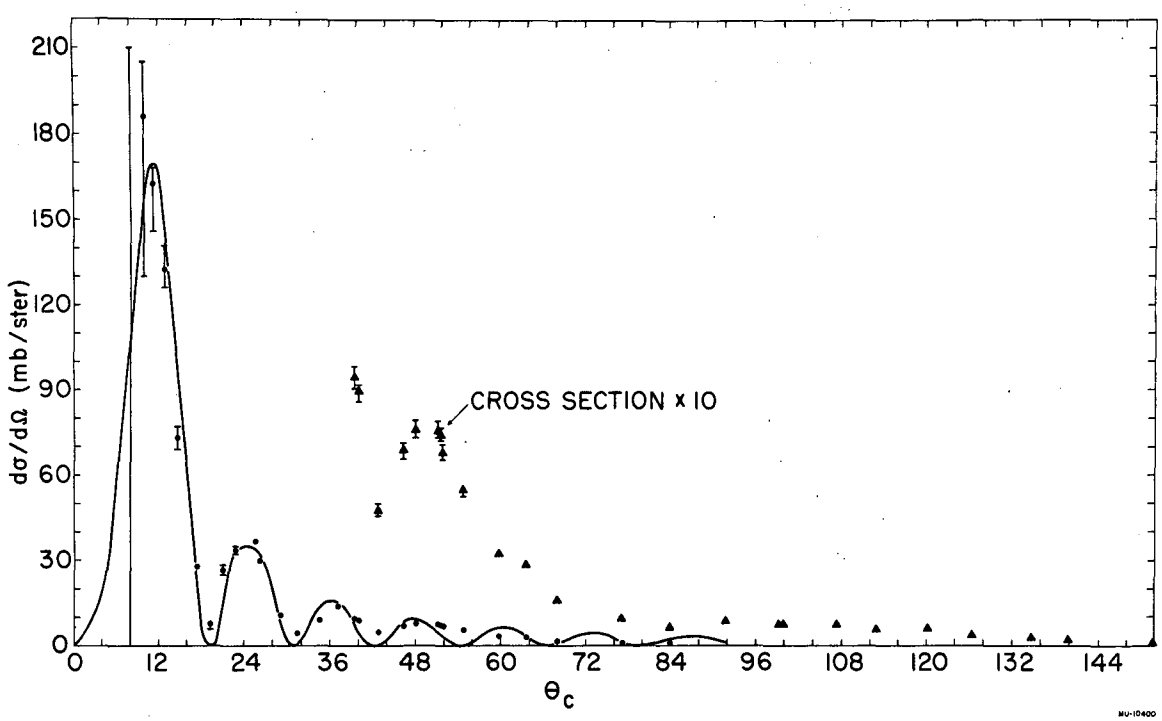

Fig. 11. Angular distribution of the differential cross section (c.m.) for the reaction $Mg^{24}(\alpha, \alpha')Mg^{24*}$, $Q = -1.368$ Mev. The solid curve is $[j_2(GR_0)]^2$ for $R_0 = 6.60 \times 10^{-13}$ cm.

with theory was made.

Conclusions

Observed angular distributions of inelastically scattered alpha particles are in partial agreement with the predictions of the ABM theory; the agreement for alpha-particle scattering is about as good as for protons inelastically scattered from the same levels. Bombardment with alpha particles may have the advantage of providing more clear-cut information about spins and parities of excited states because of the zero spin of the alpha particle. However, alpha-particle bombardment also has a definite disadvantage because of the greater difficulty of measuring the cross sections at small angles, where results are of greatest significance in comparing with theoretical predictions. Small-angle measurements are more difficult for alpha particles because the range difference between the inelastic and elastic peaks is in general smaller than for protons of comparable total range. And furthermore the elastic peak itself is larger for alpha-particle bombardment because of the greater Coulomb scattering cross section.

In any case, it would seem worth while to work out a more detailed theory of the angular distributions to be expected from inelastic alpha-particle scattering. Should such a theory be developed, the measurement of this type of angular distribution might prove to be quite a useful tool of nuclear spectroscopy.

$\alpha = 4.0026031$

Table I

Differential cross sections for the elastic scattering of 48-Mev alpha particles by carbon and ratios to the Rutherford cross sections

θ_C (deg.)	$\frac{d\sigma}{d\Omega}$ (mb per steradian)		$\frac{d\sigma}{d\Omega} \Big/ \frac{d\sigma}{d\Omega}_{Ruth.}$
9.48	4589 ± 85	230.	1.496 ± .028
10.34	3125 ± 62	160.	1.438 ± .028
11.67	2016 ± 41	100.	1.503 ± .030
13.48	1159 ± 16	58.	1.530 ± .021
14.34	643 ± 13	32.	1.085 ± .021
15.67	247.1± 4.9	12.4	0.592 ± .012
17.47	75.18± 1.3	3.8	0.2775± .0046
18.32	17.34± .42	.87	0.0774± .0019
20.12	30.36± .44	1.5	0.1961± .0028
23.43	136.3± 1.8	6.8	1.606 ± .021
26.71	126.9± 2.0	6.4	2.509 ± .039
29.53	68.18± .91	3.4	1.997 ± .027
29.99	55.95± .73	2.8	1.742 ± .023
33.26	10.27± .16	.5	0.4782± .0075
36.51	8.46± .19	.43	0.566 ± .013
36.51	8.95± .13	.45	0.5987± .0089
36.51	8.35± .13	.42	0.5585± .0084
39.28	19.24± .48	.96	1.707 ± .042
39.73	21.31± .42	1.06	1.977 ± .039
42.98	27.27± .41	1.36	3.329 ± .049
46.18	23.55± .36	1.19	3.864 ± .059
49.37	15.87± .27	.79	3.347 ± .057
52.52	9.13± .14	.46	2.426 ± .036
52.52	9.04± .14	.45	2.401 ± .036
55.23	$7.86^{+.15}_{-.20}$	.39	$2.512^{+.049}_{-.063}$
58.78	$9.72^{+.21}_{-.25}$	.49	$3.90^{+.08}_{-.10}$

Table I (Cont.)

Differential cross sections for the elastic scattering of 48-Mev alpha particles by carbon and ratios to the Rutherford cross sections

θ_C (deg.)	$\frac{d\sigma}{d\Omega}$ (mb per steradian)	$\frac{d\sigma}{d\Omega} \Big/ \frac{d\sigma}{d\Omega}_{Ruth.}$
58.78	9.34 ± .16 .45	3.746 ± .062
61.45	10.21 ± .17 .51	4.803 ± .078
64.94	10.06 ± .14 .5	5.768 ± .081
64.94	9.60 ± .14 .48	5.502 ± .078
64.94	9.76 ± .14 .49	5.595 ± .080
67.55	6.66 ± .10 .33	4.387 ± .067
70.99	2.476±.058 .12	1.935 ± .046
70.99	2.444±.047 .12	1.910 ± .037
73.56	1.208±.023 .06	1.194 ± .023
76.92	$0.916^{+.023}_{-.031}$ .045	$0.938^{+.024}_{-.032}$
76.92	0.908±.026 .045	0.931 ± .026
79.43	1.642±.035 .082	1.871 ± .040
82.72	2.131±.055 .106	2.770 ± .071
88.00	1.340±.026 .067	2.018 ± .039
88.39	1.020±.022 .05	1.632 ± .035
93.92	$0.431^{+.014}_{-.022}$ .022	$0.826^{+.027}_{-.043}$
99.30	1.142±.025 .055	2.571 ± .055
104.53	$0.981^{+.033}_{-.037}$ .049	$2.536^{+.084}_{-.095}$
109.60	$0.910^{+.028}_{-.057}$ .045	$2.66^{+.08}_{-.17}$
109.60	0.932±.023 .045	2.719 ± .066

Table II

Differential cross sections for the elastic scattering of 48-Mev alpha particles by magnesium and ratios to the Rutherford cross sections

θ_C (deg.)	$\frac{d\sigma}{d\Omega}$ (mb per steradian)	$\frac{d\sigma}{d\Omega} / \frac{d\sigma}{d\Omega}_{Ruth.}$
8.26	11230 ± 420	0.650 ± .024
9.94	5160 ± 120	0.652 ± .015
11.08	1831 ± 42	0.3646±.0084
12.83	419 ± 13	0.1476±.0046
14.57	144.6 ± 3.4	0.0855±.0020
17.40	315.5 ± 7.5	0.3739±.0089
19.23	430 ± 20	0.762 ±.035
20.98	238.2 ± 9.0	0.595 ±.022
22.75	$93.6^{+3.6}_{-2.2}$	$0.321^{+.012}_{-.008}$
25.62	4.11± .17	0.02249±.00093
26.22	4.28± .21	0.0256±.0013
29.08	48.6 ± 1.8	0.438 ±.016
31.38	51.9 ± 2.0	0.629 ±.024
34.59	$21.5^{+4.3}_{-2.2}$	$0.381^{+.076}_{-.039}$
37.11	4.35± .20	0.1011±.0046
39.44	8.24± .47	0.242 ±.014
40.06	8.13± .22	0.2539±.0069
42.79	17.55± .68	0.705 ±.027

Table II (Cont.)

Differential cross sections for the elastic scattering of 48-Mev alpha particles by magnesium and ratios to the Rutherford cross sections

θ_C (deg.)	$\frac{d\sigma}{d\Omega}$ (mb per steradian)	$\frac{d\sigma}{d\Omega} \Big/ \frac{d\sigma}{d\Omega}_{Ruth.}$
46.25	11.06 ± .43	0.597 ± .023
48.00	7.17 ± .20	0.445 ± .012
51.08	3.378 ± .087	0.2638 ± .0066
51.40	2.85 ± .14	0.228 ± .011
51.78	2.88 ± .11	0.2372 ± .0090
54.64	3.51 ± .10	0.352 ± .010
59.59	2.96 ± .17	0.409 ± .023
63.47	1.365 ± .041	0.2364 ± .0071
67.84	0.707 ± .030	0.1548 ± .0066
77.00	0.459 ± .032	0.155 ± .011
83.73	0.316 ± .032	0.141 ± .014
91.62	0.374 ± .037	0.222 ± .022
98.99	0.224 ± .022	0.168 ± .016
99.06	0.245 ± .049	0.183 ± .037
99.64	0.224 ± .022	0.170 ± .017
107.12	0.152 ± .023	0.141 ± .021
120.02	0.068 ± .014	0.084 ± .017
134.58	$0.014^{+.014}_{-.007}$	$0.022^{+.022}_{-.011}$

Table III

Differential cross sections for the reaction $C^{12}(\alpha,\alpha')C^{12*}$ (Q=-4.43 Mev) in the center-of-mass system

θ_C (deg.)	$\frac{d\sigma}{d\Omega}$ (mb per steradian)	θ_C (deg.)	$\frac{d\sigma}{d\Omega}$ (mb per steradian)
9.17	6.1 - 23.8	50.17	5.70 $^{+.12}_{-.18}$
10.53	10.7 - 31.0	53.39	8.05 $^{+.17}_{-.23}$
13.23	38.8 ± 8.3	56.13	8.50 $^{+.16}_{-.23}$
14.58	38.2 $^{+3.8}_{-7.3}$	59.74	8.27 $^{+.16}_{-.17}$
15.93	38.1 ± 3.7	62.44	7.21 $^{+.15}_{-.22}$
17.78	43.4 $^{+0.9}_{-2.1}$	65.99	5.43 $^{+.12}_{-.15}$
18.64	29.0 $^{+0.7}_{-1.7}$	68.63	4.62 $^{+.10}_{-.15}$
20.48	27.35 $^{+.55}_{-.89}$	72.11	5.28 ± .11
23.82	13.13 $^{+.30}_{-.85}$	74.71	5.59 $^{+.11}_{-.15}$
27.16	8.79 $^{+.41}_{-.47}$	78.12	6.08 $^{+.18}_{-.19}$
30.03	11.6 $^{+0.3}_{-1.3}$	80.66	5.15 $^{+.11}_{-.15}$
30.03	10.9 $^{+0.2}_{-1.0}$	83.98	4.50 $^{+.11}_{-.12}$
30.49	10.71 $^{+.22}_{-.25}$	89.30	2.976 $^{+.061}_{-.089}$
33.82	11.54 $^{+.27}_{-.48}$	89.70	3.195 $^{+.062}_{-.089}$
37.12	8.59 $^{+.18}_{-.20}$	95.26	3.093 $^{+.075}_{-.087}$
40.41	5.33 $^{+.11}_{-.23}$	100.67	3.428 $^{+.077}_{-.100}$
43.68	3.47 $^{+.07}_{-.21}$	105.92	3.68 $^{+.10}_{-.14}$
46.93	3.86 $^{+.08}_{-.15}$	111.01	3.36 $^{+.08}_{-.15}$

Table IV

Differential cross sections for the reaction $C^{12}(\alpha,\alpha')C^{12*}$ (Q=-7.65 Mev) in the center-of-mass system

θ_C (deg.)	$\frac{d\sigma}{d\Omega}$ (mb per steradian)	θ_C (deg.)	$\frac{d\sigma}{d\Omega}$ (mb per steradian)
10.67	$0^{-9.9}$	63.31	$0.480^{+.021}_{-.076}$
12.05	$0^{-6.8}$	66.89	$0.270^{+.020}_{-.072}$
13.43	$0^{-5.0}$	69.56	$0.230^{+.025}_{-.067}$
18.03	$0^{-7.3}$	73.08	$0.296^{+.017}_{-.058}$
18.90	$5.0^{+0.8}_{-1.6}$	75.71	$0.286^{+.037}_{-.053}$
20.75	$1.29^{+.10}_{-.31}$	79.16	$0.269^{+.021}_{-.075}$
24.16	$0.63^{+.05}_{-.17}$	81.71	$0.153^{+.031}_{-.052}$
27.55	$0.57^{+.04}_{-.20}$	85.07	$0.042^{+.019}_{-.008}$
30.94	$0.52^{+.03}_{-.18}$	90.83	$0^{-.033}$
34.30	$0.45^{+.02}_{-.12}$	101.86	$0^{-.085}$
37.66	$0.280 \pm .073$	112.21	$0^{-.194}$
40.99	$0.38^{+.04}_{-.11}$		
44.32	$0.30^{+.04}_{-.11}$		
47.60	$0.223^{+.018}_{-.058}$		
50.88	$0.304^{+.022}_{-.087}$		
54.14	$0.53^{+.04}_{-.16}$		
56.92	$0.56^{+.05}_{-.14}$		
60.57	$0.494^{+.032}_{-.060}$		

Table V

Differential cross sections for the reaction $C^{12}(\alpha,\alpha')C^{12*}$ (Q=-9.61 Mev) in the center-of-mass system

θ_C (deg.)	$\frac{d\sigma}{d\Omega}$ (mb per steradian)	θ_C (deg.)	$\frac{d\sigma}{d\Omega}$ (mb per steradian)
10.76	36^{+3}_{-13}	51.38	$1.76^{+.15}_{-.51}$
12.16	30^{+3}_{-11}	54.66	$1.48^{+.13}_{-.37}$
13.56	$23.7^{+2.2}_{-7.5}$	57.46	$1.48^{+.09}_{-.52}$
14.93	$20.5^{+1.7}_{-6.6}$	61.16	$1.76^{+.08}_{-.52}$
16.30	$23.2^{+2.0}_{-5.3}$	63.91	$1.53^{+.13}_{-.54}$
19.07	$18.7^{+1.6}_{-4.3}$	67.53	$1.10^{+.10}_{-.26}$
20.94	$18.0^{+0.7}_{-3.5}$	70.22	$1.11^{+.08}_{-.44}$
24.38	$13.3^{+0.4}_{-2.0}$	73.76	$1.72^{+.14}_{-.71}$
27.83	$10.3^{+0.4}_{-1.4}$	76.40	$1.67^{+.18}_{-.50}$
31.25	$7.0^{+0.2}_{-1.2}$	79.87	$1.83^{+.08}_{-.47}$
34.63	$6.6^{+0.3}_{-1.2}$	82.45	$1.99^{+.13}_{-.69}$
38.02	$5.6^{+0.2}_{-1.3}$	85.83	$2.05^{+.24}_{-.60}$
41.39	$5.61^{+.23}_{-.42}$	91.63	$2.09^{+.13}_{-.56}$
44.73	$4.2^{+0.2}_{-1.1}$	102.70	$1.65^{+.09}_{-.71}$
48.07	$2.27^{+.21}_{-.61}$	113.07	$0.99 - 1.47$

Table VI

Differential cross sections for the reaction $Mg^{24}(\alpha,\alpha')Mg^{24*}$ (Q=-1.368 Mev) in the center-of-mass system

θ_C (deg.)	$\frac{d\sigma}{d\Omega}$ (mb per steradian)	θ_C (deg.)	$\frac{d\sigma}{d\Omega}$ (mb per steradian)
8.18	0 - 210	51.20	$7.58^{+.35}_{-.24}$
9.96	186^{+19}_{-56}	51.53	7.45 ± .21
11.16	163^{+6}_{-17}	51.90	$6.78^{+.31}_{-.21}$
12.84	$132.5^{+8.5}_{-5.7}$	54.77	$5.50^{+.15}_{-.23}$
14.64	73.1 ± 4.1	59.72	3.26 ± .13
17.44	27.8 ± 1.1	63.60	$2.892^{+.077}_{-.096}$
19.28	$7.8^{+0.4}_{-2.0}$	67.98	$1.608^{+.054}_{-.042}$
21.02	26.9 ± 1.8	77.14	0.932± .036
22.79	33.5 ± 1.3	83.88	0.644± .063
25.67	36.81± .94	91.78	0.857± .037
26.26	29.94± .72	99.14	0.756± .032
29.15	$10.72^{+.52}_{-.43}$	99.22	0.756± .036
31.45	$4.29^{+.36}_{-.24}$	99.80	$0.760^{+.033}_{-.024}$
34.68	8.98± .12	107.28	$0.721^{+.048}_{-.028}$
37.19	$14.06^{+.69}_{-.49}$	112.89	0.578± .045
39.54	9.47± .38	120.18	$0.592^{+.045}_{-.022}$
40.15	$8.97^{+.24}_{-.36}$	126.38	0.350± .027
42.90	4.79± .21	134.71	0.281± .019
46.37	$6.91^{+.23}_{-.33}$	138.84	0.195± .039
48.06	7.64± .31	151.87	$0.074^{+.074}_{-.037}$

ACKNOWLEDGMENTS

It is a pleasure to thank Professor Owen Chamberlain for his patient guidance and assistance in all phases of the work. The assistance of Dr. Robert E. Ellis, Mr. Homer E. Conzett, and Mr. Robert Summers-Gill in setting up the cyclotron runs and obtaining the data is gratefully acknowledged. Mr. G. Bernard Rossi, Mr. W.B. Jones, and the other members of the 60-inch cyclotron group have provided outstanding cyclotron operation for all the runs.

This work was done under the auspices of the U.S. Atomic Energy Commission.

REFERENCES

1. R. Woods and D.S. Saxon, Phys. Rev. 95, 577 (1954); M.A. Melkanoff, J.S. Nodvik, D.S. Saxon, and R. Woods, Technical Report 7-12-55, Dept. of Physics, UCLA.
2. Conference, Brookhaven National Laboratory (January 1955) on "Statistical Aspects of the Nucleus".
3. J.S. Blair, Phys. Rev. 95, 1218 (1954)
4. N.S. Wall, J.R. Rees, and K.W. Ford, Phys. Rev. 97, 726 (1955)
5. R.E. Ellis, "Elastic Scattering of 48-Mev Alpha Particles by Heavy Nuclei", (Thesis), University of California Radiation Laboratory Report No. UCRL-3114, August 1955; R.E. Ellis and L. Schecter, Phys. Rev. (to be published)
6. E. Bleuler and D.J. Tendam, Phys. Rev. 99, 1605 (1955)
7. R.M. Eisberg, G. Igo, and H.E. Wegner, Phys. Rev. 99, 1606 (1955)
8. For example, see J.M. Blatt and V F. Weisskopf, "Theoretical Nuclear Physics", Wiley, 1952
9. S.T. Butler, Proc. Roy. Soc. (London) A208, 559 (1951)
10. R. Huby and H.C. Newns, Phil. Mag. 42, 1442 (1951)
11. N. Austern, S.T. Butler, and H. McManus, Phys. Rev. 92, 350 (1953)
12. G.E. Fischer, "The Scattering of 10-Mev Protons on Carbon and Magnesium" (Thesis), University of California Radiation Laboratory Report No. UCRL-2546 1954, and Phys. Rev. 96, 704 (1954)
13. J.W. DuMond and E.R. Cohen, Revs. Modern Phys. 25, 691 (1953)
14. For example, see L.I. Schiff, "Quantum Mechanics", McGraw-Hill, 1949, p. 164.
15. F. Ajzenberg and T. Lauritsen, Revs. Modern Phys. 27, 77 (1955)
16. K. Strauch and W.F. Titus, Phys. Rev. 95, 854 (1954)

17. H.E. Conzett, private communication.

18. G.J. Hecht, "Angular Distributions of Charged Particles from 31-Mev Protons on Carbon" (Thesis), University of California Radiation Laboratory Report No. UCRL-2969, April 21, 1955.

19. R.G. Freemantle, W.M. Gibson, and J. Rotblat, Phil. Mag. 45, 1200 (1954)

20. V.K. Rasmussen, D.W. Miller, B.M. Carmichael, and M.B. Sampson, Phys. Rev. 92, 852 (1953)

21. J. R. Holt and C.T. Young, Nature 164, 1000 (1949).